P2-80

Simulations of diffusive lithium evaporation onto the NSTX vessel walls

D. P. Stotler [a,*], C. H. Skinner [a], W. R. Blanchard [a],

P. S. Krstic [b] H. W. Kugel [a], H. Schneider [a], L. E. Zakharov [a],

[a] *Princeton Plasma Physics Laboratory, Princeton University, P. O. Box 451, Princeton, NJ 08543-0451, USA*

[b] *Oak Ridge National Laboratory, Oak Ridge, TN 37831, USA*

Abstract

A model for simulating the diffusive evaporation of lithium into a helium filled NSTX vacuum vessel is described and validated against an initial set of deposition experiments. The model consists of a three-dimensional representation of the vacuum vessel, the elastic scattering process, and a kinetic description of the evaporated atoms. Additional assumptions are required to account for deuterium outgassing during the validation experiments. The model is found to agree with the data to within the estimated errors over a range of helium pressures. However, trends in both the experimental data and simulation results suggest the presence of systematic errors.

Preprint submitted to Elsevier Science *August 24, 2010*

Key words: (PSI-19), NSTX, Lithium, Coating, DEGAS, (JNM) T0100 Theory and Modeling, L0300 Lithium

PACS: 81.15.-z, 34.50.-s, 52.65.Pp, 51.10.+y

1 Introduction

The National Spherical Torus eXperiment (NSTX, $R = 0.85$ m, $a < 0.67$ m, $R/a > 1.27$) [1] has been investigating the use of lithium as a surface coating material to improve plasma performance and to provide better control of the core plasma density. In the principal technique used thus far, lithium is evaporated from the top of the vessel via one or two evaporators (LITERs) [2] into a vacuum between discharges and is primarily deposited on the lower divertor surfaces. Lithium coatings have reduced deuterium recycling, improved confinement and suppressed ELMs [3,4]. However, in plasmas with suppressed ELMs, core carbon and medium-Z metallic impurity concentrations increase in the latter part of the discharge [4]. The temporal and spatial origin of these impurities is the subject of ongoing research, as is the search for techniques to prevent them being generated or expel them periodically. The preventive technique that we consider here is to increase the coverage of the vacuum vessel with lithium so as to reduce sputtering of impurities from the graphite tiles and metal surfaces.

* Corresponding and presenting author
Email address: dstotler@pppl.gov (D. P. Stotler).

Evaporation into a helium filled vessel accomplishes this objective via diffusion of the lithium throughout the vessel. Observations of this effect were reported previously in conjunction with evaporation during helium glow discharge cleaning [5]. The mean free path of the Li atoms scales inversely with the helium pressure, so lower pressures coat the bottom of the vessel most effectively and higher pressures lead to thicker coatings closer to the injectors at the top of the vessel. Because of the three dimensional (3-D) nature of the problem, an optimal strategy that provides a specified minimum coating thickness on all surfaces in the minimum amount of time, and with the least amount of lithium, is far from obvious. To this end, we have developed a model of this system using the 3-D Monte Carlo neutral transport code DEGAS 2 [6] that can be applied iteratively to optimize the coating procedure.

This paper describes the initial validation of this model against a set of diffusive evaporation experiments performed during the 2009 NSTX run campaign.

2 Model

The first component of the simulation model is a 3-D description of the NSTX vacuum vessel, including the two LITER evaporators used in this run campaign, as well as a surface representing the quartz microbalance (QMB) [5] that provides

the deposition data with which the model is compared.

Coordinates for most tile surfaces have been taken from engineering drawings produced during the design and construction of NSTX. In-vessel measurements made during the most recent opening of NSTX provide updated coordinates for the lower divertor tile surfaces and the crucial toroidal gaps in front of the LITER evaporators and the QMB. The toroidal variation of the model, e.g, gaps between tiles, is prescribed in DEGAS 2 with a "pie slice" method [6] in which the various structures are represented as plane figures (Fig. 1) revolved about the major axis of the torus through a range of toroidal angles (Fig. 2). This toroidal discretization need not be uniform and is adapted to provide the appropriate toroidal widths for material surfaces. The LITERs are located at toroidal angles of 45° (Bay K) and 195° (Bay F). The QMB is at 225° (Bay E).

The angular distribution of lithium atoms emitted by the LITERs measured in the laboratory [2] agrees well with a molecular flow calculation [7] made using the Cbebm code. A spline fit to the latter forms the basis for the angular distribution of the lithium source in DEGAS 2; the atoms have a thermal energy distribution with a temperature of 900 K. The LITERs are operated at a computer controlled temperature [2], and the corresponding evaporation rates are determined from the lithium vapor pressure and a molecular flow conductance calculation. Laboratory data confirm the accuracy of these rates. For the experiments described here, the

LITERs were operated at $\sim 640^\circ$ C with a corresponding evaporation rate of 60 mg/min.

The atomic physics processes in the problem are elastic scattering of lithium atoms off of helium and deuterium molecules. The latter enter as a result of significant outgassing during the evaporation process. The relative amounts of helium and deuterium in the vessel will be discussed in Sec. 3.1. The differences between the mean free paths for the two processes, given in [5], are smaller than the uncertainties in either. If we assume, in the interest of simplicity, that they are the same, we can treat the two background species (He and D_2) as one by virtue of their equal masses and temperatures. The simulated pressure is then just the sum of the helium and deuterium pressures. We assume that this pressure is uniform throughout the vessel and at room temperature (300 K). The cross section used is that of the Li-He scattering as obtained by Hamel [8], $\sigma_{\mathrm{Li-He}} = 2.49 \times 10^{-19}$ m^2; the associated mean free path is

$$\lambda_{\mathrm{Li-He}} = 9.92 \times 10^{-2}/P_{\mathrm{tot}} \text{ m}, \tag{1}$$

where the pressure is in mtorr.

The final component of the model is the assumption that the lithium atoms stick to all materials surfaces inside the vacuum vessel with 100% probability.

3 Experimental Data

The experiments providing the data for this paper were based on an initial pressure prescription for coating the vessel developed from an earlier set of DEGAS 2 simulations. The lowest pressure, 0.032 mtorr ($\lambda_{\mathrm{Li-He}} = 3.1$ m), provides the best coverage of the lower divertor and other surfaces near the bottom of the vessel. The highest pressure, 0.2 mtorr ($\lambda_{\mathrm{Li-He}} = 0.5$ m) coats the upper surfaces, although it also results in strong deposition peaks on the upper divertor plates around the LITERs. An intermediate pressure, 0.1 mtorr ($\lambda_{\mathrm{Li-He}} = 1.0$ m) is used to cover the miplane region and the primary passive plates. Apart from peaks in the coating thickness around the upper divertor, the largest departure from toroidal uniformity is on the portion of the lower center stack that is partially shadowed from both LITERs. This prescription has evaporation being performed at the lowest helium pressure for one unit of time and at the two higher pressures for two units of time each. For this experiment, the total evaporation time was selected to enable several shots to be run during the time allotted to the experiment rather than to achieve a specified lithium thickness.

The practical implementation of this evaporation prescription begins with a 2.5 mtorr helium gas fill (normally used for glow discharge cleaning). The torus pumping system was then employed to bring the pressure down to 0.2 mtorr; at the same

time the LITER evaporation began. The vessel pressure rose during this interval due to outgassing. An examination of residual gas analysis data taken during other NSTX experiments indicates that this gas is predominantly molecular hydrogen; we assume here that it is all D_2.

The pumps were turned on again at the completion of this evaporation interval to bring the vessel pressure down to 0.1 mtorr for the second evaporation period. We anticipated running the third evaporation interval at 0.03 mtorr in the same manner. However, the pressure rise from the outgassing quickly exceeded that target pressure in the two initial experiments. On the subsequent three experiments, the torus pumps were left open during the third evaporation interval.

3.1 Pressure and QMB Data

The vessel pressures were measured by an ionization gauge. Being calibrated such that its readings provide the pressure of air, a calibration factor must be applied to obtain the pressure of other gases. For D_2, this is $c_{D_2} = 0.392$; for He, $c_{He} = 0.186$. Namely, we write the ionization gauge pressure as:

$$P_{ig} = c_{He} P_{He} + c_{D_2} P_{D_2}. \tag{2}$$

Having no other means of determining the precise composition of the gas at a given point in time, we assume that after pump-down of the initial prefill, the gas

is all He. We then suppose that all pressure rise is due to outgassing of D_2 and that the gas composition remains fixed during the subsequent pumping intervals. These assumptions together with Eq. (2) are sufficient to allow P_{He}, $P_{\mathrm{D_2}}$, and $P_{\mathrm{tot}} = P_{\mathrm{He}} + P_{\mathrm{D_2}}$ to be uniquely determined. The resulting pressures for the first of the five evaporation experiments are shown together with the target helium pressures in Fig. 3.

The operation of the QMB monitors is described in [9] and [5]. The raw data from the monitors is a frequency that is directly proportional to deposited mass once the effects of temperature changes have been taken into account. If the deposits are all of the same atomic mass, as expected in this case (all lithium), this mass can be directly converted to a number of atoms and then into a deposition rate (or flux, by dividing by the area of the monitor, 1.0×10^{-4} m^2). However, to facilitate interpretation the deposited mass is usually converted to a thickness using a fixed density of 1.6 gm/cm^3, as in Fig. 3. Note that because this QMB is at the top of the vessel and relatively close to the Bay F LITER, the deposition rate is greatest at the highest pressures.

To compute that rate, the QMB data are first smoothed using a boxcar average 15 data points wide (about 1 minute). These data are then interpolated onto a time grid having a uniform spacing of 36 seconds, and the rate is computed by a finite difference derivative. The full set of experimental rates, divided by the

LITER evaporation rate, is plotted as a function of the inferred total pressure in Fig. 4. This normalized deposition rate is essentially the probability for an evaporated lithium atom to be deposited on the QMB. The "tracks" apparent in the data represent the trajectories of individual evaporation sequences, suggesting the presence of a missing parameter or systematic error (e.g., in the unfolding of the pressure data).

4 Simulations and Analysis

A set of simulations have been done at 0.032, 0.1, 0.25, and 0.3 mtorr for the purpose of comparing with these data. The resulting "baseline" normalized deposition rates are plotted in Fig. 4.

The uncertainty in the depth of the QMB below the secondary passive plates is estimated to be 1 cm. The corresponding variation in the normalized deposition rate is 3% using data from a separate simulation with the QMB shifted downward by 1 cm. The simulated QMB is assumed to point downward, although its precise orientation has not been measured. We estimate that its angle relative to horizontal is $< 30^\circ$ and that the associated uncertainty in the deposition rate scales as the cosine of that angle, that is, $< 13\%$. For simplicity, we combine these two uncertainties into a single figure of 10%.

The uncertainty in the location of the QMB within the gap between the surrounding plates is also estimated to be 1 cm, even though the width of the gap has been explicitly measured. In this case, the sensitivity of the normalized deposition rate can be found using data from adjacent toroidal segments in the simulations. An average deviation of 10% is found from the resulting data points.

The location of the LITERs in their operating position is not precisely known, even though the locations of points on the surrounding tiles has been measured. Two sensitivity simulations were carried out in which the LITERs were moved radially outward within this tile gap by 6 mm. The deposition rate in these simulations was about 28% lower than in the baseline runs. Most of this drop is due to increased deposition (from 8% to 33% at 0.25 mtorr) on the backs and sides of the tiles adjacent to the LITERs.

The gas pressure and scattering cross sections both enter the problem only through the mean free path. Consequently, we can use the variation of the deposition rate with pressure (nearly linear, according to Fig. 4) to assess its sensitivity to the cross section. For these low interaction energies ($\ll 1$ eV), resonances and other quantum effects introduce significant variations ($> 10\%$) in the momentum transfer cross sections [10] with small changes in the interaction energy. Quantum oscillations introduce even larger isotopic dependencies, up to 50%, in the case that a signficant fraction of the outgassing is H_2 or HD. We have also introduced errors by treating

scattering of He and D_2 with a single cross section and ignoring angular dependence of the scattering. We account for all of these effects with a single uncertainty of 50%.

The relative fraction of He and D_2 in the vessel is not known and can only be estimated using the model described in Sec. 3.1. This translates into an uncertainty in the total pressure (the input to the simulations) since the measured quantity is the ionization gauge reading and not the total pressure. The ionization gauge calibration factors are such that variations in the assumptions used in that model lead to changes in the total pressure on the order of 40%.

A final, possibly significant, error may result from operating the LITERs at temperatures above 600° C. Under these conditions, the evaporated lithium in the LITER snout may no longer be in the molecular flow regime used to estimate the evaporation rate and compute the angular distribution of emitted atoms. The conductance of the snout in this case would be expected to increase strongly with the lithium vapor pressure, and consequently, with temperature. The corresponding enhancement in the evaporation rate beyond that predicted by the molecular flow formula could be a factor of two, or even more. Note that an increased evaporation rate would reduce the measured normalized deposition rate, exacerbating the disparity with the simulation results seen in Fig. 4. On the other hand, a departure from molecular flow might result in a more centrally peaked angular distribution

for the atoms that would act in the other direction. Because of the magnitude and complexity of these considerations, we do not account for them in the remaining analysis.

The above uncertainties are all independent so that we can sum their squares to obtain a total error of 71% in the simulations. The error bars in Fig. 4 are actually $\sqrt{2/\pi}$ of this value, as is suggested by the validation metric in [11].

The experimental data were divided into 0.01 mtorr wide bins around the simulated pressure values; the resulting mean values are shown in Fig. 4. Ninety percent confidence intervals were then computed for the experimental data [11] and added to the plot as error bars. However, because of the large number of experimental points ($\sim$ 100) in each bin, these confidence intervals are too small to be discerned in the figure. On the other hand, the experimental errors in the bins are not normally distributed about the mean values, as is assumed in the derivation of the confidence intervals. Consequently, these intervals should be treated with skepticism.

The simulation results agree with the experimental data within the estimated uncertainties. Nonetheless, the consistent 50% discrepancy between the simulated rates and the experimental points, as well as the "tracks" apparent in the experimental data, suggest the presence of a hidden parameter or systematic error

that needs to be identified. To this end, we plan dedicated experiments that will decouple the components of the model. For example, we can operate the LITERs separately, utilize QMBs in other parts of the vessel, and run the LITERs at lower temperatures. The uncertainties can also be reduced with additional in-vessel measurements and the use of a baratron pressure gauge.

5 Conclusions

In conclusion, we have developed a model for predicting and optimizing the coating of the NSTX vessel with lithium via diffusive evaporation into a helium filled vessel. The results of the validation effort described here point to the most significant uncertainties in the model and suggest experiments for more discriminating validation experiments.

Acknowledgments

This work supported by U.S. DOE Contracts DE-AC02-09CH11466 and DE-AC05-00OR22725. The authors wish to thank C. Priniski for the in-vessel spatial calibration data used in this work.

References

[1] M. Ono et al., Nucl. Fusion 40 (2000) 557.

[2] H. W. Kugel et al., Phys. Plasmas 15 (2008) 056118.

[3] R. Maingi et al., Phys. Rev. Lett. 103 (2009) 075001.

[4] M. G. Bell et al., Plasma Phys. Control. Fusion 51 (2009) 124054.

[5] C. H. Skinner et al., J. Nucl. Mater. 390–391 (2009) 1005.

[6] D. P. Stotler et al., J. Nucl. Mater. 290–293 (2001) 967.

[7] D. P. Stotler, T. D. Rognlien, S. I. Krasheninnikov, Phys. Plasmas 15 (2008) 058303.

[8] W. A. Hamel et al., J. Phys. B: At. Mol. Phys. 19 (1986) 4127.

[9] C. H. Skinner et al., J. Nucl. Mater. 363–365 (2007) 247.

[10] P. S. Krstic, D. R. Schultz, J. Phys. B: At. Mol. Opt. Phys. 42 (2009) 065207.

[11] P. W. Terry et al., Phys. Plasmas 15 (2008) 062503.

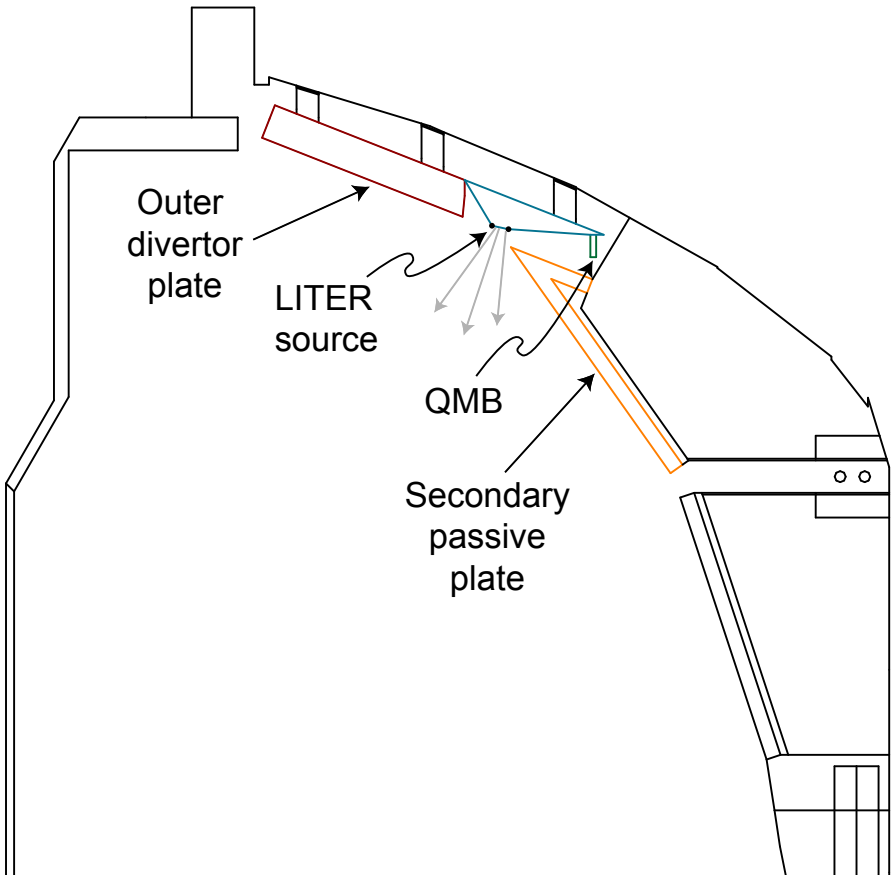

Figure 1. Poloidal plane figures used to construct the vacuum vessel elements in the model.

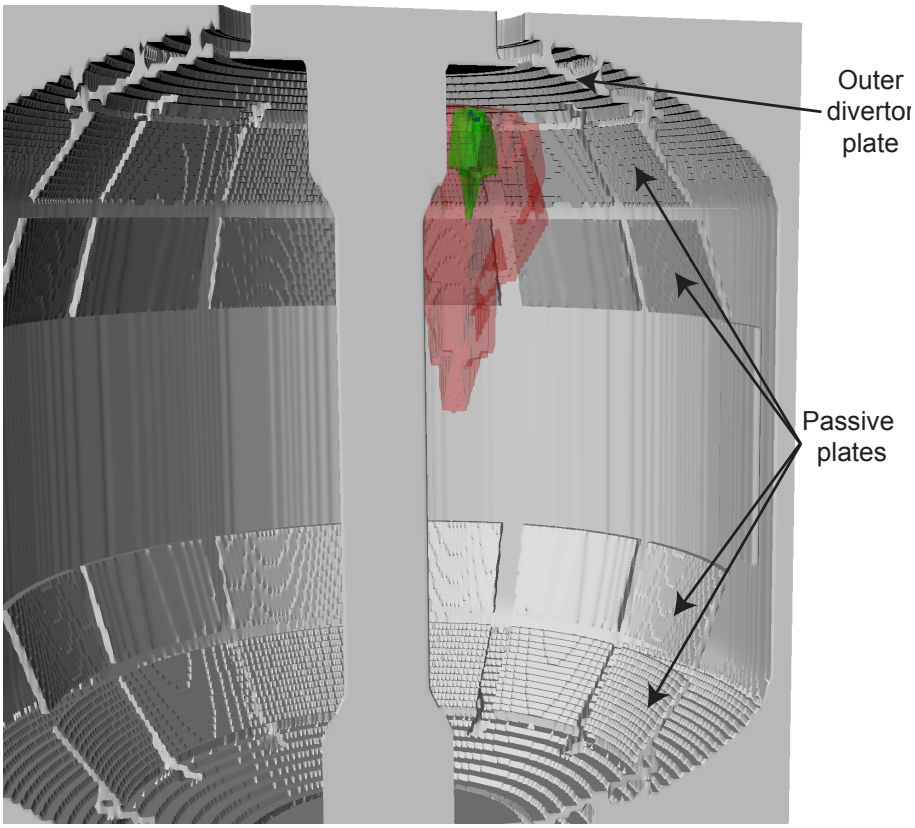

Figure 2. Three-dimensional rendering of the vacuum vessel elements in the model. Two lithium density contours associated with the Bay F LITER are also included. The apparent corrugation of the surfaces, especially the outer divertor plate, is an artifact of the method used to generate the plot and is not present in the computational model.

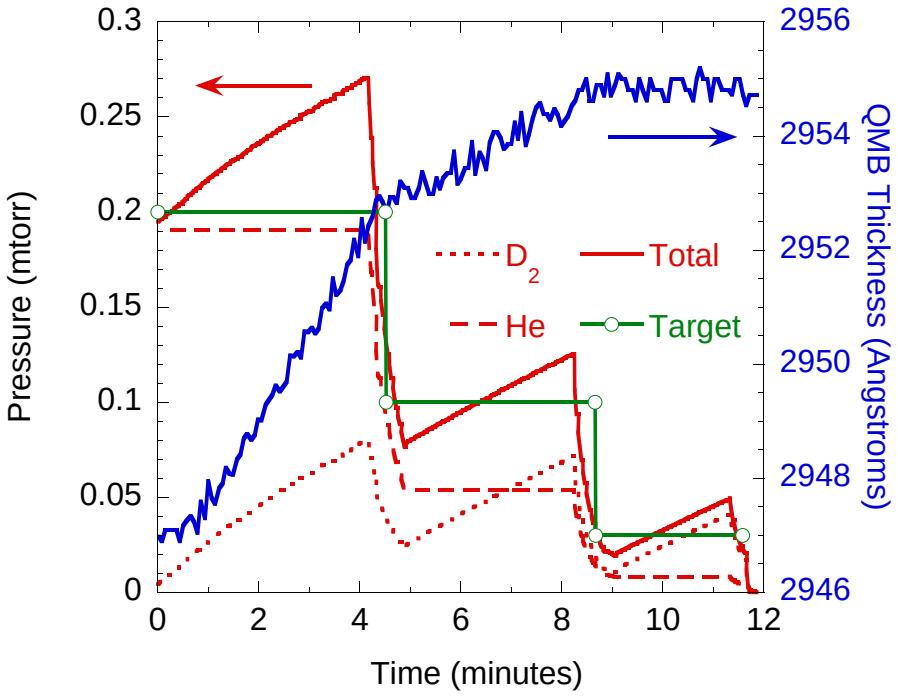

Figure 3. Pressure and QMB data from shot 135697. The "Target" points indicate the prescribed helium pressures. The actual helium, deterium, and total pressures are inferred from the experimental ionization gauge data via the model described in Sec. 3.1. The corresponding QMB thickness data are overlaid (right axis).

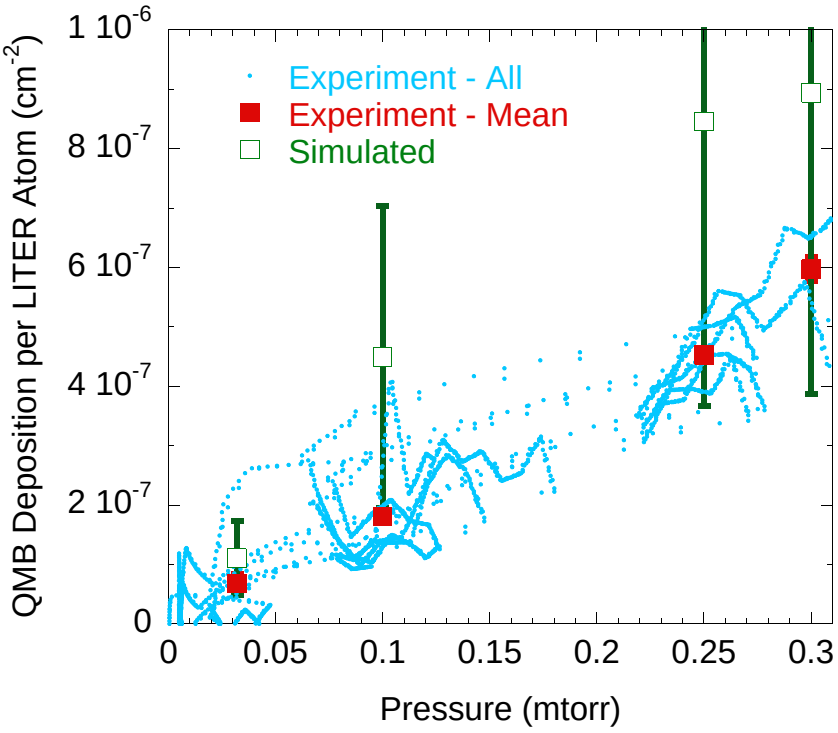

Figure 4. The lithium deposition rate on the QMB, normalized by the total LITER evaporation rate, is plotted as a function of the total (He and D_2) pressure. All of the experimental data are shown as small points. The filled squares are the means of these data at the pressures used in the simulations. Confidence intervals for the experimental data are plotted as error bars, but cannot be discerned on this scale. The simulated data are plotted as open squares with error bars determined as described in the text.